Instability of the shear layer in the near wake of a circular cylinder*

SHEN Kaiquan, DONG Genjin and LU Xiyun**

(Department of Mechanics and Mechanical Engineering, University of Science and Technology of China, Hefei 230026, China)

Received August 13, 2002; revised October 8, 2002

Abstract The instability of the shear layer separated from a circular cylinder is studied with the Reynolds number (Re) of 3000 $\sim 10^4$ by numerically solving the two-dimensional Navier-Stokes equations. In the wake of the cylinder, primary vortex shedding with natural frequency f_s occurs, and the instability of the shear layer with frequency f_t develops, which leads to mixing layer eddies and interacts with the primary shedding vortices. However, there remains some uncertainties regarding to the variation of the shear layer characteristic frequency with the Reynolds number. Based on the previous experimental work, several relationships of f_t/f_s with Re has been proposed including $f_t/f_s \sim Re^{0.5}$ by Bloor, $f_t/f_s \sim Re^{0.87}$ by Wei and Smith and $f_t/f_s \sim Re^{0.67}$ by Prasad and Williamson. The objective of this study is to predict reasonably the relation of the shear layer instability frequency with the Reynolds number based on the present accurate calculation with the high-order schemes and high-resolution spectrum analysis. According to our calculated results, a variation for the normalized shear-layer frequency of the form $f_t/f_s \sim Re^{0.69}$ is predicted numerically, which is in good agreement with a recent experimental measurement of $Re^{0.67}$ and physical prediction of $Re^{0.7}$.

Keywords: **shear layer instability, vortex shedding, circular cylinder flow.**

The study of the transition to turbulence and the wake formation behind a bluff body has received a great deal of attention owing mainly to its theoretical and practical significance. Although a number of investigations[1,2] have addressed the transition and instability of the shear layer separating from a circular cylinder, there remains some uncertainty regarding the shear layer characteristic frequency. In particular, the variation of the shear layer characteristic frequency with the Reynolds number has a surprising scatter in the literature.

Over the past decades, some investigations have addressed diverse aspects of shear-layer instability. Roshko[3] first observed experimentally the existence of a transition regime in the wake of the cylinder and found distinct irregularities in the wake velocity fluctuation. He showed that there exist three different regimes of the flow at low to moderate Reynolds number, which are the laminar, transition and irregular turbulent regimes. Then Bloor[4] carried out the systematic measurements of the characteristic frequency associated with the shear-layer instability (f_t), in analogy with the instability observed in wall boundary layers. Subsequent investigators have used a variety of terminology including the Kelvin-Helmholtz frequency and the secondary frequency. Based on parameter variations similar to those of laminar boundary layers, Bloor[4] suggested that f_t/f_s should scale with $Re^{0.5}$, where f_s represents the Karman vortex shedding frequency. Since then, other investigators including Wei and Smith[5], Kourta et al.[6], Norberg[7] and Fey et al.[8] have measured the shear-layer frequency. Many of these investigators attempted to fit their data to the $Re^{0.5}$ variation, although an examination of their actual data points does not support such a variation. Wei and Smith[5] found that the normalized shear-layer frequency f_t/f_s varies with $Re^{0.77}$ from hot-wire measurements and with $Re^{0.87}$ from flow visualization. They surmised that the former technique of measurement would inherently result in lower values of the shear-layer frequency, because the intermittent shear-layer fluctuations produce spurious peaks in the spectrum in the frequency domain. Norberg[7] suggested that a single power law may not represent the variation of f_t/f_s over the entire Reynolds number ranging up to $Re = 10^5$ and found that a local maximum in the exponent occurs at $Re = 5000$. Recently, Prasad and Williamson[9,10] performed experiments to investigate the instability of

* Supported by the National Natural Science Fund for Distinguished Scholars (No. 10125210), the Innovation Projects of the Chinese Academy of Sciences (CAS) (Grant No. KJCX-SW-L04, KJCX2-SW-L2), and the Hundred Talents Programme of CAS

** To whom correspondence should be addressed. E-mail: xlu@ustc.edu.cn

the shear layer separating from a circular cylinder, and carried out a least-squares analysis by using both their experimental data and all of the previously available data to produce a variation of $f_t/f_s \sim Re^{0.67}$. It therefore appears from the above discussion that the variation of the normalized shear-layer frequency with the Reynolds number remains an unresolved problem.

A large number of numerical studies have been devoted to the analysis of the unsteady flow around a circular cylinder with the low and moderate Reynolds number regimes[11~16]. However, very little numerical investigation has been performed on the instability of the shear layer separating from the sides of a circular cylinder. Braza et al.[17] first calculated the two-dimensional Navier-Stokes equations to illustrate the generation of the mixing layer vortices in the separated shear layers past the circular cylinder and assessed their shedding frequency related to the fundamental frequency in the Reynolds number of $2000 \sim 10^4$. They proposed f_t/f_s varies with $Re^{0.5}$, which is consistent with the prediction by Bloor[4]. Recently, Ling et al.[18] solved the two-dimensional Navier-Stokes equations by using vortex method and finite-difference method at $Re = 3000 \sim 10^4$ and predicted the behavior of the normalized shear-layer frequency f_t/f_s varying with $Re^{0.87}$. On the other hand, based on simple physical arguments that account for the variation of the characteristic velocity and length scales of the shear layer, Prasad and Williamson[9,10] predicted a variation for the normalized shear-layer frequency of the form $Re^{0.7}$. Furthermore, it is possible to predict the existence of an absolute instability by the linear stability theory, but there is no theoretical study concerning the development of the shear-layer instability in the near wake of the circular cylinder. Thus, the reasonable prediction of the variation of the normalized shear-layer frequency with the Reynolds number is still needed through an accurate numerical calculation.

Here, we firstl discuss the basic physical mechanisms of the instability of the shear layer separated from a circular cylinder, which provides some guidance to our computation. The shear layer separated from a cylinder becomes unstable at $Re \sim 10^3$. The shear layer instability due to the action of a Kelvin-Helmholtz mechanism has a length scale of the thickness of the separating shear layer, which is generally smaller than the characterized length (e.g. the cylinder diameter). Consequently, the length and time scales of the shear layer instability are much smaller than those of the wake instability. As argued by Williamson[19], the shear layer instability necessarily needs to develop and to then undergo significant amplification before the shear layer rolls up to form the primary vortex. Thus, a critical Reynolds number Re_c, below which shear layer instability would not be perceived, may occur. Based on the experiments in Prasad and Williamson[9,10], it has been found that $Re_c \approx 1200$ for parallel shedding conditions along a three-dimensional cylinder, whereas $Re_c \approx 2600$ for oblique shedding conditions. In the present calculation, in order to capture the shear layer frequency efficiently, we choose the Reynolds number ranging from 3000 to 10^4.

On the other hand, there still remains an important question regarding the spanwise structure of the shear-layer instability, in particular on whether the shear layer instability waves are always parallel to the axis of the cylinder, or if indeed the waves adopt the spanwise structure of the Karman vortices. From the recent experiments performed by Prasad and Williamson[9,10], it is found that the instability of the separated shear layer is on the whole two-dimensional along the span, this is in agreement with the suggestion of Braza et al.[17]. It, therefore, appears that the most unstable mode in the shear layer is two-dimensional, despite the fact that the base flow may be in the parallel shedding case or in the oblique shedding case. Thus, the two-dimensional Navier-Stokes equations are calculated to deal with the shear-layer instability and the normalized shear-layer frequency.

A numerical study of the instability of the shear layer separating from the sides of a circular cylinder is performed to accurately predict the normalized shear-layer frequency with the Reynolds number by solving the two-dimensional incompressible Navier-Stokes equations. A second-order accurate in time fractional step method is employed to advance temporal derivative, and a third-order biased-upwind scheme[20] and a fourth-order central scheme approximations are used to discretize the convective terms and viscous terms, respectively. To accurately identify the frequencies, a high-resolution power spectrum analysis is used to capture the frequencies. According to our calculated results, the normalized shear-layer frequencies and the flow patterns are analyzed and discussed.

1 Mathematical formulation

The governing equations are the two-dimensional incompressible Navier-Stokes equations. To non-dimensionalize the governing equations, we use the radius of the cylinder R as the length scale; the uniform free-stream velocity U as the velocity scale. Then the non-dimensional governing equations are given in polar coordinates (r, θ) as follows:

$$\frac{\partial u}{\partial r} + \frac{u}{r} + \frac{1}{r}\frac{\partial v}{\partial \theta} = 0, \tag{1}$$

$$\frac{\partial u}{\partial t} + u\frac{\partial u}{\partial r} + v\frac{\partial u}{r\partial \theta} - \frac{v^2}{r} = -\frac{\partial p}{\partial r} + \frac{2}{Re}\left(\nabla^2 u - \frac{2}{r^2}\frac{\partial v}{\partial \theta} - \frac{u}{r^2}\right), \tag{2}$$

$$\frac{\partial v}{\partial t} + u\frac{\partial v}{\partial r} + v\frac{\partial v}{r\partial \theta} + \frac{uv}{r} = -\frac{\partial p}{r\partial \theta} + \frac{2}{Re}\left(\nabla^2 v + \frac{2}{r^2}\frac{\partial u}{\partial \theta} - \frac{v}{r^2}\right), \tag{3}$$

where $Re = 2UR/\nu$, ν is the kinematic viscosity; u and v are the dimensionless radial and circumferential velocity components, respectively; p is the dimensionless pressure; and the Laplace operator, ∇^2, is

$$\nabla^2 = \frac{\partial^2}{\partial r^2} + \frac{1}{r}\frac{\partial}{\partial r} + \frac{1}{r^2}\frac{\partial^2}{\partial \theta^2}. \tag{4}$$

In the present calculation, we use the no-slip and no-penetration boundary conditions for velocity on the wall of the cylinder. Far from the cylinder, we use the Neumann boundary condition because the far field boundary is sufficiently far from the cylinder so that the effect of the cylinder is neglected. In the circumferential direction, we use periodic boundary conditions.

2 Numerical methods

To describe the numerical method clearly, the Navier-Stokes equations are written in vector form,

$$\frac{\partial \boldsymbol{V}}{\partial t} = -\nabla p + \boldsymbol{L} + \boldsymbol{N}, \tag{5}$$

where $\boldsymbol{V}$ is the velocity vector, $\boldsymbol{N}$ represents the convective terms and $\boldsymbol{L}$ denotes the viscous terms.

A fractional step method is employed to discretize the governing equations in time. In this approach, we first obtain an intermediate velocity, $\hat{\boldsymbol{V}}$, by omitting pressure and using the second-order Adams-Bashforth scheme on the convective terms and the Crank-Nicolson scheme on the viscous terms,

$$\frac{\hat{\boldsymbol{V}} - \boldsymbol{V}^n}{\Delta t} = -\frac{1}{2}(3\boldsymbol{N}^n - \boldsymbol{N}^{n-1}) + \frac{1}{2}\boldsymbol{L}^n, \tag{6}$$

where the superscripts refer to the time step. This intermediate velocity is corrected by pressure to obtain a second intermediate velocity, $\tilde{\boldsymbol{V}}$, from

$$\frac{\tilde{\boldsymbol{V}} - \hat{\boldsymbol{V}}}{\Delta t} = -\nabla p^{n+1/2}. \tag{7}$$

Finally, the velocity at time step $n+1$ is obtained from

$$\frac{\boldsymbol{V}^{n+1} - \tilde{\boldsymbol{V}}}{\Delta t} = \frac{1}{2}\boldsymbol{L}^{n+1}. \tag{8}$$

To determine the pressure p, we apply the continuity equation, which must be satisfied at the end of each complete time step. So, we take the divergence of Eq. (8) to get

$$\nabla \cdot \tilde{\boldsymbol{V}} = 0. \tag{9}$$

Then, we take the divergence of Eq. (7) and apply Eq. (9) to get

$$\nabla^2 p^{n+1/2} = \frac{\nabla \cdot \hat{\boldsymbol{V}}}{\Delta t}, \tag{10}$$

where $p^{n+1/2}$ is obtained through Eq. (10) and with the solution for $\hat{\boldsymbol{V}}$ from Eq. (6). Then $\tilde{\boldsymbol{V}}$ and $\boldsymbol{V}^{n+1}$ can be calculated from Eqs. (7) and (8). No boundary conditions are necessary for either of the two intermediate velocities, and the boundary conditions on velocity are applied to get the velocity at the next time step.

By solving Eq. (10), a pressure boundary condition must be implemented. To control the time-splitting error, we use the consistent scheme developed by Karniadakis et al.[11] on boundary conditions for pressure on solid boundaries where velocity vanishes,

$$\frac{\partial p}{\partial n} = -\frac{2}{Re}\boldsymbol{n} \cdot \nabla \times (\nabla \times \boldsymbol{V}), \tag{11}$$

where $\boldsymbol{n}$ is the unit vector normal to the wall.

In this study, a staggered grid, which is uniformly spaced in the circumferential direction and is exponentially stretched in the radial direction, is employed for the discretization of the governing equations. To approximate the space derivatives, a third-order biased-upwind scheme[20] and a fourth-order central scheme approximations are used to discretize the convective terms and viscous terms respectively.

3 Results and discussion

To accurately capture the shear layer instability with much smaller length and time scales, a high grid resolution is needed. We have taken numerical test with several different grid numbers of 256×256, 512×256 and 512×384 in the radial (r) and circumferential (θ) directions. The number of mesh points for

the calculations was finally chosen as 512×384. The computational domain was $30R$ in the radial direction, and time step was 0.0005. The convergence check with different grid sizes and time steps has been extensively performed in our previous work[15, 16, 21~24]. It has been determined that the computed results are independent of the time steps and the grid sizes.

To illustrate the computational procedure, only some typical results are mainly discussed. The computational global parameters (e.g. Strouhal number, lift and drag coefficients) of circular cylinder flows are evaluated. Fig. 1 shows the variations of the lift and drag coefficients (i.e. C_L and C_D) versus time at $Re = 5000$ and 8000. The corresponding mean values of C_D are 1.18 and 1.20 approximately, the Strouhal numbers St ($= 2f_s$, here St is defined based on the non-dimensional length of the cylinder diameter) are 0.22 and 0.21, and the root-mean-square (rms) values of the lift coefficients C_{Lrms} are about 0.78 and 0.79, respectively. It is found that those results are in good agreement with some typical experimental data[3~6] and computational results[17, 23].

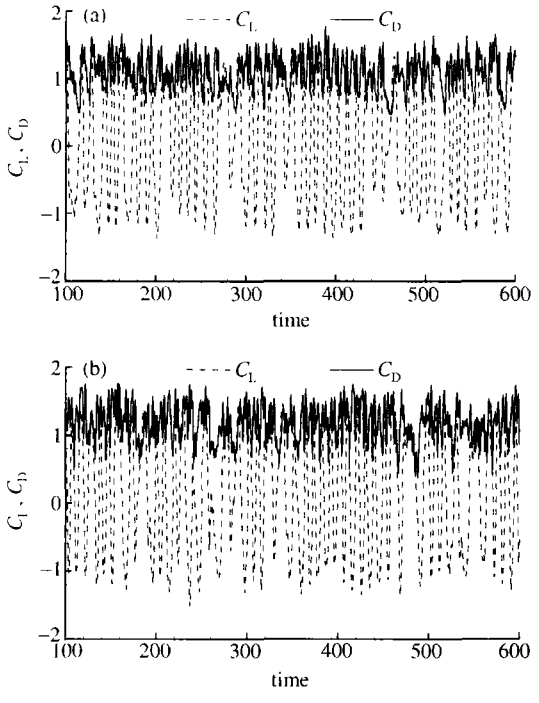

Fig. 1. Variation of the lift and drag coefficients versus time. (a) $Re = 5000$; (b) $Re = 8000$.

Instantaneous streamlines and vorticity contours are shown in Fig. 2 for $Re = 8000$ at $t = 382$ and 382.6. The flow patterns clearly show the development of large-scale structures in the near wake and secondary eddies near the wall. It can be identified that the separated shear layers develop and undergo significant amplification before the shear layer rolls up to form the primary vortex. These small-scale eddies, named mixing layer vortices[9, 10, 17], result from the Tollmein-Schlichting instability occurring in the separated mixing layers. The instability frequency is shown in the following spectrum analysis. To demonstrate the effect of the Reynolds number on the flow patterns, Fig. 3 shows the instantaneous streamlines and vorticity contours at $Re = 3000$. By comparing Fig. 2 with 3, it is seen that the formation of the separated shear layers and the appearance of the mixing layer vortices are clearly exhibited at higher Reynolds numbers, which is consistent with experimental visualization of Williamson's[19], who found that the shear layer instability would be developed and amplified when the Reynolds number was higher than a critical Reynolds number Re_c.

To identify the instability frequency, the spectral analysis is performed on the numerically obtained time-dependent signals of the pressure and velocity along the separating mixing layer. In order to take accurate evaluation of frequencies, the spectral resolution is equal to 0.001. In the wake of the cylinder, vortex shedding with natural frequency f_s occurs and the instability of the separated shear layer with frequency f_t appears. As reported previously[6, 25], suppressing or attenuating of the eddies can be achieved by using a splitter plate, and the transition mechanism leading to the frequency f_t develops independently on the vortex shedding mechanism at the frequency f_s. Hence it is reasonable to suppose that the mechanism leading to f_t is due to the generating of the natural frequency in a free shear layer[1, 2, 26].

Here, some typical results of the spectral analysis are discussed. Fig. 4 shows the spectrum power density (PSD) of the pressure and the velocity at $Re = 4000$. The existence of peaks at frequencies f_s and f_t is clearly shown in the spectra. Although the spectra are calculated based on the pressure and the velocity, even at different locations, the peaks of f_s and f_t as well as of the frequencies due to their interaction are consistent with each other. Because of the nonlinear effect, the simultaneous interaction of f_s and f_t, which are incommensurate frequencies, leads to generation of new predominant frequencies, such as the superharmonic components of f_s (i.e. $2f_s$, $3f_s$,

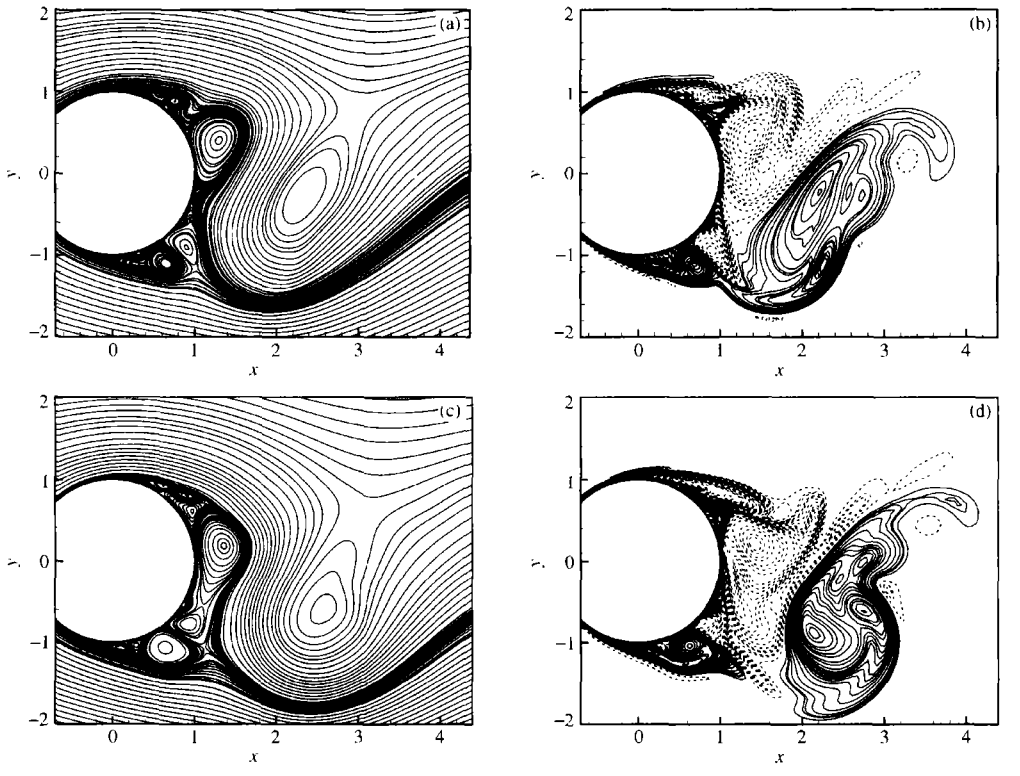

Fig. 2. Instantaneous streamlines and vorticity contours at $Re = 8000$. (a) Streamlines at $t = 382$; (b) vorticity contours at $t = 382$; (c) streamlines at $t = 382.6$; (d) vorticity contours at $t = 382.6$. Solid lines, positive values; dashed lines, negative values.

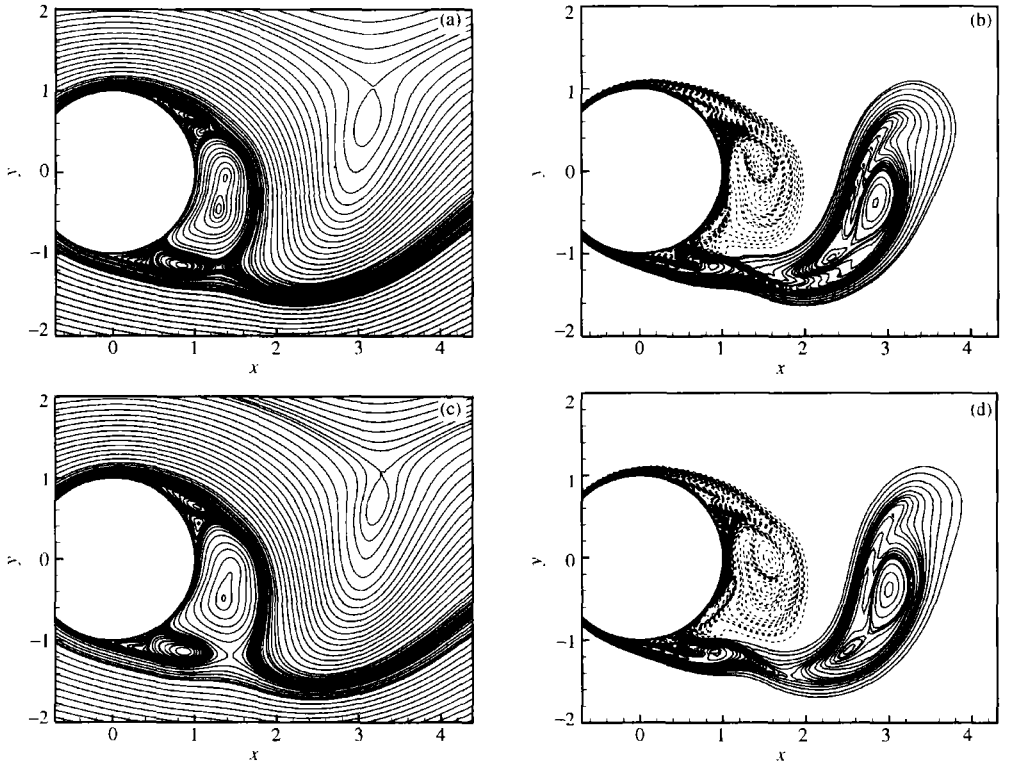

Fig. 3. Instantaneous streamlines and vorticity contours at $Re = 3000$. (a) Streamlines at $t = 382.4$; (b) vorticity contours at $t = 382$; (c) streamlines at $t = 382.6$; (d) vorticity contours at $t = 382.6$.

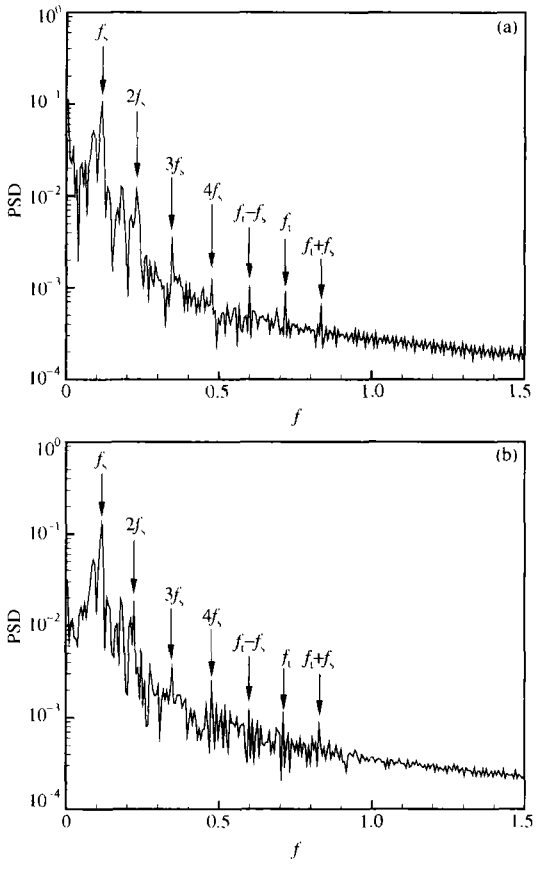

Fig. 4. Spectrum power density (PSD) of the pressure and the velocity at $Re = 4000$. (a) The pressure at (1.50, 1.10); (b) the velocity at (−0.16, 1.07).

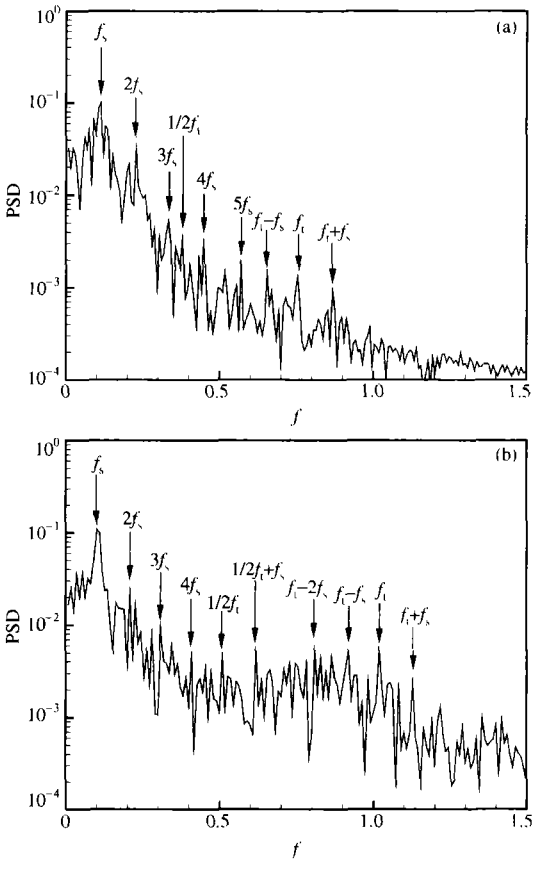

Fig. 5. Spectrum power density (PSD) of the pressure. (a) The pressure at (0.50, 1.10) for $Re = 5000$; (b) the pressure at (0.24, 1.10) for $Re = 8000$.

etc.), $f_t \pm f_s$ and so on. The interaction is typical of what happens in a free shear layer under the action of an external forcing frequency, as reported in experiments[5,6,10] and computations[1,2,17,18,26]. In the present case, the natural vortex shedding frequency f_s should be considered as the forcing frequency acting upon the separated mixing layer with the frequency f_t. The development of the mixing layer eddies is strongly related with the instability frequency f_t, in the same way as the peak at f_s corresponds to the development of the vortex shedding in the cylinder wake. To further demonstrate the instability frequency and the interaction between the natural vortex shedding and mixing layer eddies, Fig. 5 shows the spectra of the pressure at $Re = 5000$ and 8000. The peaks of f_s and f_t as well as the frequencies due to their interaction are clearly shown in the spectra. Due to the vortex pairing in the mixing layer, which was also found in previous work[17,18,26], the peak at the subharmonic component $f_t/2$ exists, and the peaks of the interaction between $f_t/2$ and f_s appear.

According to the spectra analysis, the vortex shedding frequency f_s and the instability frequency f_t can be accurately predicted. Table 1 lists the values of the ratio f_t/f_s, which are compared with previous experimental results[4−6, 10]. By using a least-square analysis for the present calculated results, the variation of f_t/f_s can be approximately expressed as $f_t/f_s \sim 0.01976Re^{0.69}$ (shown in Fig. 6). Thus we predict a variation for the ratio $f_t/f_s \sim Re^{0.69}$, which is in good agreement with a recent experimental measurement of $Re^{0.67}$ and physical prediction of $Re^{0.7}$ by Prasad and Williamson[9,10], but somewhat different from $Re^{0.5}$ by Bloor[4] and $Re^{0.87}$ by Wei and Smith[5].

Table 1. Values of the frequency-ratio f_t/f_s

Re	Present results f_t/f_s	Bloor $f_t/f_s = 0.095Re^{0.5}$	Wei and Smith $f_t/f_s = (Re/470)^{0.87}$	Prasad and Williamson $f_t/f_s = 0.023Re^{0.67}$
4000	6.10	6.01	6.44	6.09
5000	7.17	6.71	7.82	7.07
8000	9.88	8.50	11.76	9.69
10000	11.37	9.50	14.30	11.25

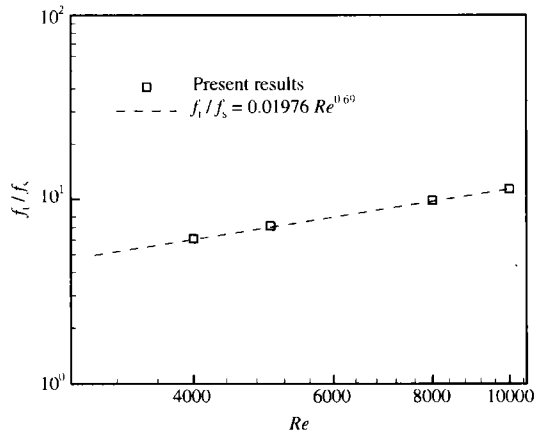

Fig. 6. Variation of the ratio of the instability frequency and the vortex shedding frequency with Reynolds number.

We include all the available experimental data[4-7,10,27,28] of the ratio f_t/f_s and arrive at the variation displayed in Fig. 7. The lines of the predictions by Bloor[4], Wei and Smith[5] and Prasad and Williamson[10] are plotted in Fig. 7. It is clear that a power law of the form $Re^{0.69}$, suggested by using the present calculations, reasonably represents the variation of the ratio f_t/f_s and is consistent with the recent experimental measurement $Re^{0.67}$ by Prasad and Williamson[9,10]. Although some numerical simulations have been performed to deal with the separated shear layer instability frequency[17,18], it is the first time to establish that $f_t/f_s \sim Re^{0.69}$ based on accurate calculations with high mesh resolution and higher-order spatial schemes.

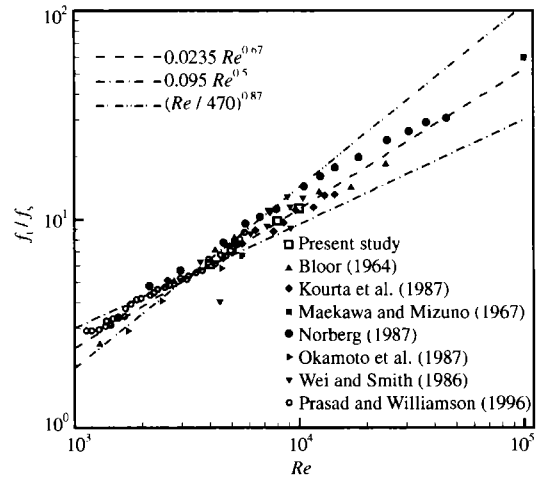

Fig. 7. Variation of the ratio of the instability frequency and the vortex shedding frequency including all the available experimental data with Reynolds number.

Acknowledgements The authors are grateful to Prof. Ling Guocan at the Institute of Mechanics of the Chinese Academy of Sciences for helpful discussion.

References

1 Ho, C. M. et al. Perturbed free shear layers. Ann. Rev. Fluid Mech., 1984, 16: 365.
2 Huerre, P. et al. Local and global instabilities in spatially developing flows. Ann. Rev. Fluid Mech., 1990, 22: 473~537.
3 Roshko, A. On the drag and shedding frequency of two-dimensional bluff bodies. NACA Tech. Note 3169, 1954.
4 Bloor, M. S. The transition to turbulence in the wake of a circular cylinder. J. Fluid Mech., 1964, 19: 290.
5 Wei, T. et al. Secondary vortices in the wake of circular cylinders. J. Fluid Mech., 1986, 169: 513.
6 Kourta, A. et al. Nonlinear interaction and the transition to turbulence in the wake of a circular cylinder. J. Fluid Mech., 1987, 181: 141.
7 Norberg, C. An experimental investigation of the flow around a circular cylinder: influence of aspect ratio. J. Fluid Mech., 1994, 258: 287.
8 Fey, U. et al. A new Strouhal-Reynolds-number relationship for the circular cylinder in the range $47 < Re < 2 \times 105$. Phys. Fluids, 1998, A2: 1547.
9 Prasad, A. et al. The instability of the separated shear layer from a bluff body. Phys. Fluids, 1996, 8: 1347.
10 Prasad, A. et al. The instability of the shear layer separating from a bluff body. J. Fluid Mech., 1997, 333: 375.
11 Karniadakis, G. E. et al. Three-dimensional dynamics and transition to turbulence in the wake of bluff objects. J. Fluid Mech., 1992, 238: 1.
12 Zhang, H. et al. On the transition of the circular cylinder. Phys. Fluids, 1995, 7: 779.
13 Henderson, R. D. Nonlinear dynamics and pattern formulation in turbulent wake transition. J. Fluid Mech., 1997, 352: 65.
14 Persillon, H. et al. Physical analysis of the transition to turbulence in the wake of a circular cylinder by three-dimensional Navier-Stokes simulation. J. Fluid Mech., 1998, 365: 23.
15 Lu, X. Y. et al. Calculation of the timing of vortex formation from an oscillating cylinder. J. Fluids Structures, 1996, 10: 527.
16 Lu, X. Y. et al. A numerical study of flow past a rotationally oscillating circular cylinder. J. Fluids Structures, 1996, 10: 829.
17 Braza, M. et al. Prediction of large-scale transition features in the wake of a circular cylinder. Phys. Fluids, 1990, A2: 1461.
18 Ling, G. C. et al. Transition waves and nonlinear interactions in the near wake of a circular cylinder. Science China (A), 1997, 40: 849.
19 Williamson, C.H.K. Vortex dynamics in the cylinder wake. Ann. Rev. Fluid Mech., 1996, 28: 477.
20 Rai, M. M. et al. Direct simulations of turbulent flow using finite-difference schemes. J. Comput. Phys., 1991, 96: 15.
21 Lu, X. Y. Numerical study of the flow behind a rotary oscillating circular cylinder. Int. J. Comput. Fluid Dyn., 2002, 16: 65.
22 Lu, X. Y. et al. A large eddy simulation of the near wake of a circular cylinder. Acta Mechanica Sinica, 2002, 18: 18.
23 Lu, X. Y. et al. Application of large eddy simulation to flow past a circular cylinder. ASME J. Offshore Mech. Arctic Engng., 1997, 119: 219.
24 Lu, X. Y. et al. Application of large eddy simulation to an oscillating flow past a circular cylinder. ASME J. Fluids Engng., 1997, 119: 519.
25 Unal, M. F. et al. On vortex shedding from a cylinder. Part 2. Control by splitter-plate interference. J. Fluid Mech., 1988, 190: 513.
26 Wu, J. Z. et al. Post-stall flow control on an airfoil by local unsteady forcing. J. Fluid Mech., 1998, 371: 21.
27 Maekawa, T. et al. Flow around the separation point and in the near-wake of a circular cylinder. Phys. Fluids, 1967, S184.
28 Okamoto, S. et al. The effect of sound on the vortex-shedding from a circular cylinder. Bull. JSME, 1981, 24: 45.